Cell, Vol. 115, 705–713, December 12, 2003, Copyright ©2003 by Cell Press

The Bacterial Cytoskeleton: An Intermediate Filament-Like Function in Cell Shape

Nora Ausmees, Jeffrey R. Kuhn, and Christine Jacobs-Wagner*
Department of Molecular, Cellular, and Developmental Biology
Yale University
New Haven, Connecticut 06520

Summary

Various cell shapes are encountered in the prokaryotic world, but how they are achieved is poorly understood. Intermediate filaments (IFs) of the eukaryotic cytoskeleton play an important role in cell shape in higher organisms. No such filaments have been found in prokaryotes. Here, we describe a bacterial equivalent to IF proteins, named crescentin, whose cytoskeletal function is required for the vibrioid and helical shapes of *Caulobacter crescentus*. Without crescentin, the cells adopt a straight-rod morphology. Crescentin has characteristic features of IF proteins including the ability to assemble into filaments in vitro without energy or cofactor requirements. In vivo, crescentin forms a helical structure that colocalizes with the inner cell curvatures beneath the cytoplasmic membrane. We propose that IF-like filaments of crescentin assemble into a helical structure, which by applying its geometry to the cell, generates a vibrioid or helical cell shape depending on the length of the cell.

Introduction

How cells create and maintain a defined shape is a fundamental problem from bacteria to humans. The eukaryotic cytoskeleton, which consists of microtubules, actin microfilaments, and intermediate filaments, determines the various cell shapes of higher organisms. A multitude of cell shapes is also encountered in the prokaryotic world. The shape of a bacterial cell is often a conserved trait for a given species or genus and has been widely used as a taxonomical characteristic. This is apparent in the names of some bacteria, such as *Helicobacter* (helical), *Vibrio* (vibrioid), *Stella* (star), and *Caulobacter crescentus* (crescent) to name a few. Yet, little is known about the molecular mechanisms involved in cell shape determination in bacteria. In some walless bacteria, such as spiral-shaped *Spiroplasma*, an unconventional cytoskeleton is involved in motility and cell shape deformation (Townsend et al., 1980; Trachtenberg and Gilad, 2001; Trachtenberg et al., 2003). However, *Spiroplasmas*, like other mollicutes, are highly unusual bacteria in that they lack a rigid cell wall and are enveloped only by a membrane containing cholesterol, a rare component in prokaryotes. In most bacteria, cell shape maintenance requires the integrity of the exocellular wall whose rigidity and strength are primarily conferred by a crosslinked glycopeptide polymer known as peptidoglycan (or murein) (Vollmer and Holtje, 2001). This is illustrated in the classical experiment in which the degradation of the peptidoglycan of rod-shaped *E. coli* with lysozyme (in an isotonic solution to prevent cell lysis) results in a spherical cell morphology (Henning et al., 1972). Furthermore, mutations in several genes involved in peptidoglycan metabolism have been shown to alter the cell morphology of various bacteria (Henriques et al., 1998; Nelson and Young, 2000; Shohayeb and Chopra, 1987; Spratt, 1975; Tamaki et al., 1980). The involvement of the peptidoglycan in cell shape and the lack of conspicuous intracellular filaments led to the assumption for decades that cell-walled bacteria are devoid of a cytoskeleton that supports cell shape.

Studies on *Escherichia coli* and *Bacillus subtilis* have, however, shown that MreB, a protein with weak sequence similarity to actin (Bork et al., 1992), is essential for determining the rod shape of these bacteria as depletion of MreB induces the formation of rounded, inflated cells (Jones et al., 2001; Wachi et al., 1987). Despite the limited sequence conservation, MreB remarkably resembles actin at the structural level and assembles into protofilaments with a subunit repeat similar to that of F-actin, indicating that MreB and actin share a common prokaryotic ancestor (van den Ent et al., 2001). In *B. subtilis* and *E. coli*, MreB filaments form helical, filamentous structures that encircle the cell beneath the cytoplasmic membrane (Carballido-Lopez and Errington, 2003; Jones et al., 2001; Kruse et al., 2003; Shih et al., 2003). Recent evidence suggests a coupling between the biosynthesis of the peptidoglycan and the bacterial actin-like cytoskeleton (Daniel and Errington, 2003).

However, because cell shape has been mostly studied in straight rod-shaped species, it still remains unclear how more complex and often asymmetric shapes can be achieved in bacteria. Here, we identify a fibrous element of the bacterial cytoskeleton that is required for determining the vibrioid or helical shapes of *Caulobacter crescentus*. This cytoskeletal protein, here named crescentin, generates cell curvature by forming intracellular filaments similar to eukaryotic intermediate filaments at one lateral side of the cell.

Results and Discussion

Identification of Crescentin, an Essential Determinant of the Curved and Helical Shapes of *C. crescentus*

To identify the cell shape determinants of the environmental, crescent-shaped (vibrioid) bacterium *C. crescentus* (Figure 1A), we performed a visual screen of a library of random transposon (Tn*5*) insertion mutants and identified two mutant clones with a straight-rod morphology (Figure 1B). The two independent Tn*5* insertions were mapped 228 bp downstream (strain CJW761) and 15 bp upstream (strain CJW762) of the start codon of predicted open reading frame CC3699, now designated *creS*, which encodes crescentin (to refer to its involve-

*Correspondence: christine.jacobs-wagner@yale.edu

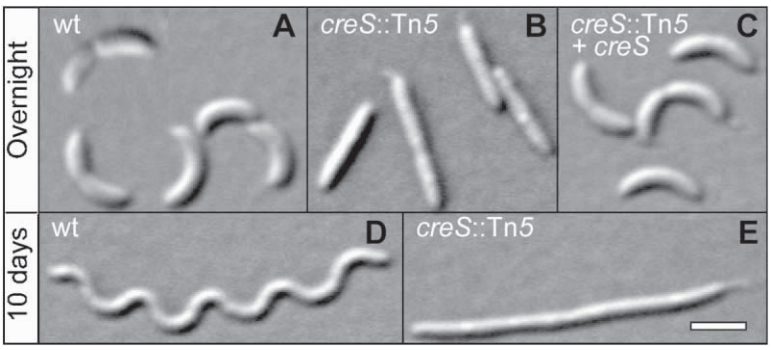

Figure 1. Crescentin Is an Essential Determinant of Vibrioid and Helical Shapes in *C. crescentus*

DIC light micrographs of the wild-type strain CB15N (wt) from an overnight culture (A) and a 10-day-old stationary phase culture (D). Cells of a *creS*::Tn*5* strain from an overnight culture (B) and a 10-day-old culture (E). The *creS*::Tn*5* strain harboring wild-type *creS* in a low-copy plasmid (C). Scale bar is equal to 2 μm.

ment in crescent-shaped cell morphology). Since the gene immediately downstream of *creS* is transcribed in the opposite direction, a polar effect on downstream gene expression by the Tn*5* insertion was ruled out. Transduction of the *creS*::Tn*5* mutation from strain CJW761 into wild-type CB15N resulted in a *creS*::Tn*5* strain (CJW763) with a straight-rod cell shape, indicating that the loss of the vibrioid shape was associated with the insertion of Tn*5* into *creS*. Introduction of a low-copy plasmid carrying wild-type *creS* into the transduced *creS*::Tn*5* mutant restored the vibrioid morphology (Figure 1C). Thus, the *creS* gene encodes an essential determinant of the vibrioid shape of *C. crescentus*.

Although the vibrioid shape is observed under most laboratory and natural growth conditions, *C. crescentus* is also known to elongate and adopt a helical cell morphology after an extended period of time in stationary phase (Wortinger et al., 1998). Figure 1D shows elongated spiral-shaped cells from a 10-day-old stationary phase culture of wild-type CB15N grown in rich medium (note that the spiral has been flattened by immobilization on the agarose pad of the slide). In contrast, the *creS*::Tn*5* mutant grown under the same conditions formed straight cell filaments (Figure 1E). Thus, crescentin is required for both the vibrioid and helical shapes of *C. crescentus*.

Crescentin Forms a Filamentous Structure that Colocalizes with the Inner Cell Curvature

Crescentin is a 430-residue protein. Most of its sequence has a distinct 7-residue repetitive pattern predicted to form coiled-coils (Lupas, 1996). Coiled-coils are the main structural elements of many fibrous proteins in eukaryotes. This, together with the involvement of crescentin in shape determination, suggested that crescentin may support shape by forming an intracellular filament. To visualize the localization of crescentin, a strain (CJW932) was engineered to replace wild-type *creS* by a chromosomal *creS-flag* construct encoding a derivative of crescentin with a short C-terminal FLAG tag. The CreS-FLAG fusion was fully functional as indicated by the vibrioid cell morphology of the *creS-flag* strain in overnight cultures (Figure 2A). Immunofluorescence microscopy with anti-FLAG antibodies on cells stained with DAPI (a DNA stain that in *C. crescentus* stains the diffuse nucleoid which fills the entire cell) revealed that functional CreS-FLAG formed a continuous pole-to-pole filament along the concave side of the cells (Figure 2A). To ensure that the localization result with CreS-FLAG was not due to an artifact of fixation, we constructed a GFP fusion to the C terminus of crescentin for its visualization in live cells. CreS-GFP was not functional on its own, but in the presence of wild-type, untagged crescentin (CreS), a functional CreS-GFP/CreS hybrid structure was formed and colocalized with the FM 4-64 membrane dye at the inner curvature of the vibrioid-shaped cells (Figures 2B–2D). The fluorescent signal from the hybrid CreS-GFP/CreS structures appeared discontinuous at places because only the CreS-GFP subunits of the hybrid structure could be visualized by fluorescence microscopy. Cells of this merodiploid *creS-gfp creS* strain (CJW815) carrying one chromosomal copy each of *creS* and *creS-gfp* were about 90% vibrioid and 10% rod-shaped after overnight growth. Similar localization results were obtained with a merodiploid strain (CJW935) carrying untagged crescentin and a GFP fusion to the N terminus of crescentin (data not shown).

Consistent with its largely wild-type cell morphology in young cultures (Figure 2B), the merodiploid *creS-gfp creS* strain differentiated into long helical cell filaments in old cultures (Figure 2E). In these cells, a CreS-GFP/CreS structure invariably followed the shortest helical path along the inner cell curvatures (Figure 2E). Analysis by optical sectioning and three-dimensional (3D) deconvolution indicated that the hybrid CreS-GFP/CreS structure was a left-handed helix (Figure 2F) whose subcellular localization is shown schematically in Figure 2G. Thus, crescentin forms helical structures in vivo at a cellular location consistent with a cytoskeletal function involved in cell curvature.

The Subcellular Localization of the Crescentin Filamentous Structure Is Important for Causing Cell Curvature

The asymmetric subcellular localization of crescentin structures (Figure 2) not only demonstrates at the molecular level the existence of cell polarity along the short axis of a bacterium, but it is also likely to pertain to the cytoskeletal function of crescentin in cell curvature. This notion was supported by experiments that used a *creS-gfp* or *gfp-creS* strain carrying CreS-GFP or GFP-CreS as the only copy of crescentin. In the absence of wild-type crescentin, CreS-GFP was not functional as indicated by the straight-rod shape of the *creS-gfp* cells from overnight or 10-day-old cultures (Figures 3A and

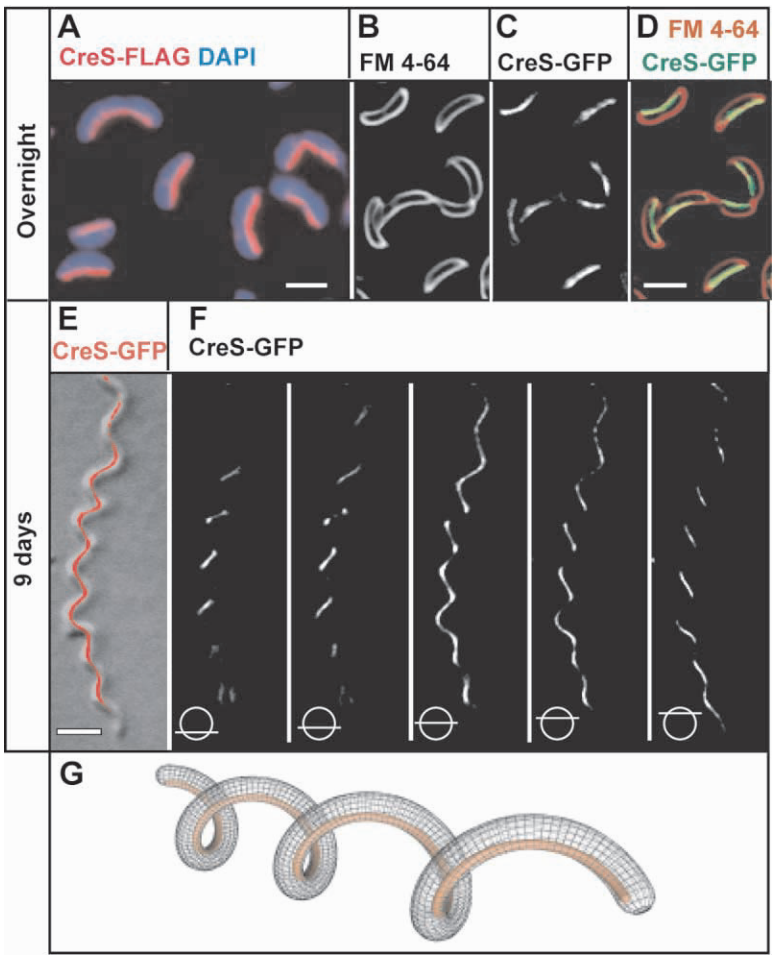

Figure 2. Functional Derivatives of Crescentin Localize Near the Membrane Specifically at the Inner Curvatures of the Cells

(A) Immunofluorescence micrograph of the *creS-flag* strain producing a functional CreS-FLAG fusion as the only crescentin protein, shown as an overlay of anti-FLAG staining (secondary antibody conjugated to FITC, red) and DAPI staining (which highlights the entire cell, blue). Scale bar is equal to 2 μm.

(B) Fluorescent image of cell membranes of merodiploid *creS-gfp creS* cells stained with FM 4-64.

(C) Fluorescent image of the CreS-GFP/CreS hybrid structure from cells in (B).

(D) Overlay of (B, green) and (C, red). Scale bar is equal to 2 μm.

(E) Overlay of DIC and GFP (red) images of a merodiploid *creS-gfp creS* cell from a 9-day-old culture. Scale bar is equal to 2 μm.

(F) Five separate optical sections along the Z-axis of the cell in (E) after deconvolution showing the CreS-GFP/CreS structure as a left-handed helix. The bottom and top sections are 700 nm apart.

(G) Schematic representation of a left-handed helical structure of crescentin localizing at the inner curvatures of a spiral-shaped cell. Three-dimensional modeling was carried out with Mathematica using a microscopic image of a helical *C. crescentus* cell as a template.

3E). In overnight cultures, CreS-GFP was still able to assemble into curved filamentous structures, but these structures appeared to be randomly localized inside the cells (Figures 3B–3C). Similar results were obtained with the *gfp-creS* strain (data not shown).

To investigate the position of the CreS-GFP filamentous structures relative to the membrane, we collected stacks of optical sections of *creS-gfp* cells stained with the FM 4-64 membrane dye and removed the out-of-focus fluorescence using a 3D deconvolution algorithm (Figure 3D). Parts of the CreS-GFP filament often colocalized with the membrane stain. However, at several occasions, the in-focus CreS-GFP signal was clearly observed at some distance from the membrane signal in the middle cross-section of the cell (Figure 3D). This is unlike the functional CreS-GFP/CreS hybrid structure whose in-focus signals invariably overlapped with the membrane stain along one lateral side of the merodiploid *creS-gfp creS* cells (Figures 2B–2D). This suggests that in the straight-rod-shaped *creS-gfp* cells, the nonfunctional CreS-GFP structures fail to form a productive (direct or indirect) interaction with the membrane, which in turn may prohibit cell curvature from occurring.

In filamentous *creS-gfp* cells from 10-day-old cultures, the nonfunctional CreS-GFP structures elongated into zigzag-shaped filaments, suggestive of a helical structure (Figures 3E–3G). Three-dimensional deconvolution of image stacks of optical sections (Figure 3H) and 3D reconstruction (Figure 3I) demonstrated the predominantly left-handed structure of the CreS-GFP helices. Right-handed helices of CreS-GFP were also observed at a low frequency (7/110). The pitch of the helical repeat (shown by the double-headed arrow in Figure 3H), was remarkably constant within the same helix and from helix to helix (1.6 ± 0.1 μm, n = 386). Thus, in the absence of wild-type crescentin, GFP fusions to crescentin retain the ability to assemble into regular helical structures in vivo, but fail to induce cell curvature, suggesting that the bulky GFP tag prevents a productive interaction between the helical structures and the cells. This also suggests that in the wild-type situation, the helical crescentin structure applies its helical geometry to the cells (as depicted in Figure 2G), presumably via a direct or indirect interaction with the cytoplasmic membrane.

Crescentin Is a Bacterial Cytoskeletal Protein Similar to Eukaryotic Intermediate Filament Proteins

Taken together, the essential function of crescentin in determining vibrioid and helical shapes, the ability of functional derivatives of crescentin to form helical structures in vivo, the colocalization of these structures with the inner curvatures of the cells, and the close proximity

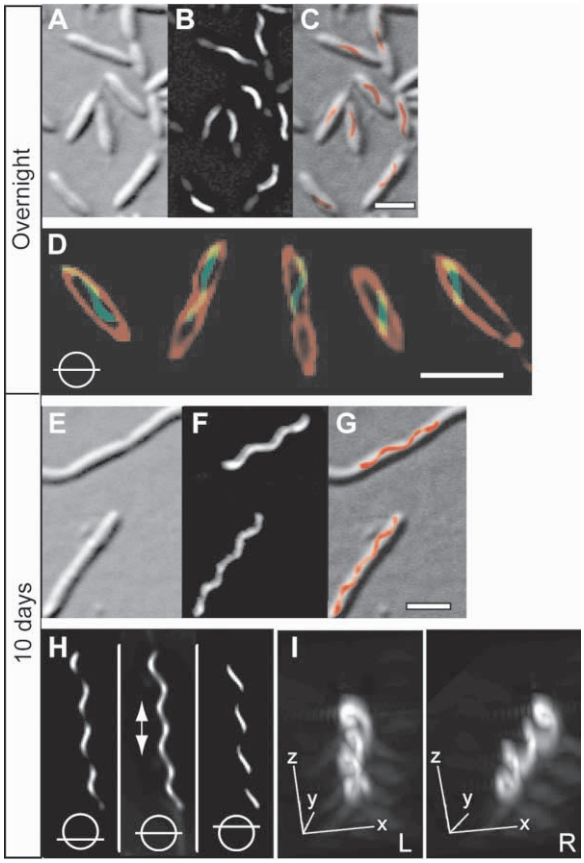

Figure 3. In the Absence of Wild-Type CreS, CreS-GFP Forms Nonfunctional Filamentous Structures that Mislocalize in the Cells

(A) DIC image of *creS-gfp* cells from an overnight culture.

(B) Corresponding fluorescent image of (A) showing curved fibrous structures formed by CreS-GFP.

(C) Overlay of (A) and (B) with the CreS-GFP signal shown in red. Scale bar is equal to 2 μm.

(D) Optical sections corresponding to the middle of *creS-gfp* cells in which the in-focus fluorescent signal of parts of the CreS-GFP structures (green) were clearly distant from the membrane signal (red), indicating that nonfunctional CreS-GFP structures have a localization defect. Scale bar is equal to 2 μm.

(E) DIC image of *creS-gfp* cells from a 10-day-old culture. Only parts of two adjacent elongated cells are shown.

(F) Corresponding fluorescent image of (E).

(G) Overlay of (E) and (F) with the CreS-GFP signal shown in red. Scale bar is equal to 2 μm.

(H) Three different optical sections (bottom, middle and top) along the Z-axis of a CreS-GFP filament after deconvolution, revealing its 3D nature as a left-handed helix. The bottom and top sections are 300 nm apart.

(I) Three-dimensional reconstruction of the CreS-GFP helix in (H). A stereo pair of the image, separated by 9 degrees for parallel viewing, is presented. Each axis represents 1 μm.

of these structures to the cytoplasmic membrane are strongly supportive of a cytoskeletal or cytoskeleton-associated role for crescentin in cell curvature.

Interestingly, crescentin shares sequence similarity with intermediate filament (IF) proteins, which play an essential cytoskeletal role in cell shape maintenance in higher eukaryotes. For example, the sequence of crescentin shares 25% identity and 40% similarity (over 254 residues) with that of cytokeratin 19, and 24% identity and 40% similarity (over 397 residues) with that of nuclear lamin A. However, such sequence similarity can be misleading because the sequences of crescentin and IF proteins largely consist of a regular 7-residue repetitive pattern of alternating hydrophobic and polar residues (heptad repeat) that forms coiled-coils. Moreover, IF proteins have no known enzymatic or nucleotide binding activity that can provide a discernible sequence signature. Thus, proteins rich in coiled-coil motifs, even those without cytoskeletal function, tend to share sequence similarity with IF proteins. However, further analysis of the sequence of crescentin using different coiled-coil and secondary structure prediction algorithms (Lupas, 1991, 1996; Rost and Sander, 1993) suggest that crescentin also share common principles of domain organization with animal IF proteins, which have been well characterized. Figure 4 shows the predicted domain organization of crescentin and compares it with two human IF proteins, cytokeratin 19 and nuclear lamin A (Figure 4). Animal IF proteins contain a large α-helical central "rod" domain flanked by so-called "head" and "tail" domains of variable size and sequence. The segmented structure of the central rod domain, which consists of four coiled-coil segments connected by short variable linkers, is a conserved feature of all types of animal IF proteins (Strelkov et al., 2003). Similarly, crescentin has a large central coiled-coil region, which can be subdivided into four distinct coiled-coil segments (Figure 4). Another structurally relevant feature of animal IF proteins is a discontinuity in the heptad repeat pattern, called "stutter," whose position in the C-terminal coiled-coil segment is highly conserved among vertebrate and invertebrate IF proteins (Brown et al., 1996; Herrmann et al., 1999; Strelkov et al., 2002). A stutter is also present in crescentin at a similar position (Figure 4).

The most distinctive property of IF proteins is their in vitro ability to form filaments ranging from 8 to 15 nm in diameter without a requirement for divalent cations, nucleotides, or other exogenous factors (Domingo et al., 1992). Because of the high insolubility of IFs, in vitro assembly of IFs first requires the solubilization of the IF protein in a strong denaturating agent (Domingo et al., 1992). Filaments are obtained by simply dialyzing the protein against physiological or low-ionic strength buffers at a neutral pH (Renner et al., 1981; Steinert et al., 1976). Similarly, a purified polyhistidine-tagged version of crescentin (His-CreS; Figure 5A) spontaneously self-assembled into filaments with a width of about 10 nm after removal of 6 M guanidinium by dialysis against a 50 mM Tris-HCl buffer at pH 7.0 (Figure 5B). Under our experimental conditions, a slight heterogeneity in the width of the His-CreS filaments was observed. These His-CreS filaments also had a tendency to laterally associate into small bundles, as it is observed for some IF proteins. The formation of His-CreS filaments was severely impeded in buffers at pH 8.4 and above. This behavior is common for IF proteins (Huiatt et al., 1980; Ip et al., 1985). Thus, crescentin has the defining biochemical property of IF-related proteins to self-assemble into filaments in vitro without the need for energy or cofactors.

In toto, crescentin is a bacterial cytoskeletal protein that is remarkably similar to animal IF proteins in many

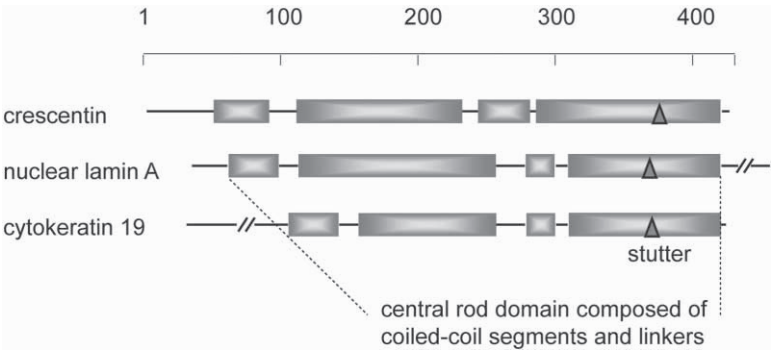

Figure 4. Crescentin and Eukaryotic IF Proteins Share Similar Domain Organization

The predicted domain architecture of crescentin is schematically shown together with that of two human IF proteins, cytokeratin 19 and nuclear lamin A. The gray rectangles show α-helical segments predicted to form coiled-coils. Cytokeratin 19 represents vertebrate cytoplasmic IF proteins in which the second coiled-coil segment is shorter than in both invertebrate cytoplasmic IF proteins and nuclear lamins.

important aspects including primary sequence and domain organization, in vitro polymerization properties, formation of filamentous structures in vivo, and biological function.

An Intermediate Filament-Like Cytoskeletal Function Required for Cell Curvature

In the absence of crescentin, *C. crescentus* cells lose their vibrioid or helical shape and resemble straight rods (Figures 1B and 1E). The bacterial rod shape is thought to require MreB, the bacterial ancestor of actin (Bork et al., 1992; van den Ent et al., 2001) because in rod-shaped *E. coli* and *B. subtilis*, loss of MreB results in a spheroid cell morphology (Jones et al., 2001; Wachi et al., 1987). Consistently, MreB is also involved in cell shape in *C. crescentus* where it forms membrane-associated actin-like cables (J. Gober, personal communication), similar to those observed in *B. subtilis* and *E. coli* (Daniel and Errington, 2003; Jones et al., 2001; Kruse et al., 2003; Shih et al., 2003). Thus, MreB and crescentin are both required for the characteristic shape of *C. crescentus*, which is reminiscent of the involvement of both actin filaments and IFs in the cell shape of higher organisms. Based on the *creS*::Tn*5* phenotype, we propose that in *C. crescentus*, MreB is essential for determining the straight rod shape whereas crescentin confers the vibrioid or helical shape of the rod.

How does crescentin mediate a vibrioid or helical cell shape? Our results suggest a mechanism that involves the in vivo helical nature of the crescentin structure, the asymmetric subcellular distribution of this crescentin structure, and the size of the cell. In this proposed mechanism, IF-like filaments of crescentin assemble into a helical structure that directly or indirectly associates with the cytoplasmic membrane specifically at one lateral side of the cell. Applying the helicity of the crescentin structure to the cell results in a vibrioid or helical cell shape depending on the size of the cell. Cells shorter than the helical pitch of the crescentin structure, such as those present in young cultures, become vibrioid whereas cells longer than the helical pitch, such as those from old cultures, become helical (spiral-shaped). To obtain the helical growth of the cells from aged cultures, the function of crescentin must be coordinated with the cell cycle and the biosynthesis of the peptidoglycan. Supporting this idea, inhibition of cell division with the β-lactam antibiotic cephalexin (which primarily interferes with peptidoglycan synthesis at the site of constriction) gradually disrupts the subcellular localization of the crescentin structure, resulting in the formation of relatively straight filamentous cells with occasional bends where the crescentin structure remains colocalized with cell curvature (our unpublished data). A connection between the function of an MreB homolog and peptidoglycan synthesis has also been proposed recently (Daniel and Errington, 2003), suggesting that the final shape of a bacterium may be achieved by the interplay between cytoskeletal and exoskeletal elements.

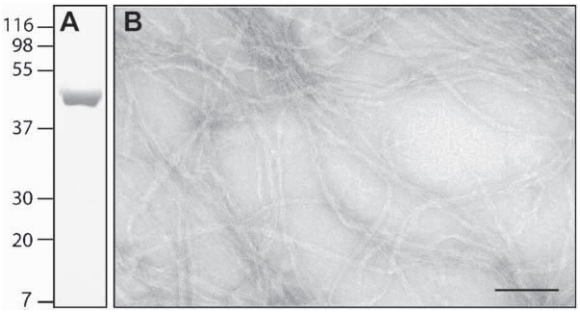

Figure 5. In Vitro Self-Assembly of His-CreS into Filaments

(A) Analysis of purified His-CreS (5 μg) by SDS-PAGE and Coomassie blue staining. Molecular size markers are indicated on the left in kilodaltons.

(B) Electron micrograph of negatively stained His-CreS filaments. The protein (0.5 mg/ml) was dialyzed against 50 mM Tris-HCl, pH 7.0 for 2 hr at room temperature. Scale bar is equal to 100 nm.

Why Is *C. crescentus* Curved?

The diversity of cell shape in the bacterial world brings the intriguing question of its biological significance. What may be the selective advantage for *C. crescentus* to be curved? We found that the *creS*::Tn*5* mutant was motile, had no detectable cell division or chromosome segregation defects based on DIC microscopy and DAPI staining, grew normally in rich and minimal media, and sustained viability in prolonged stationary phase cultures at a fairly normal rate, even when grown in competition with wild-type cells (data not shown). However, this may be a mere reflection of the "friendly" laboratory conditions. In nature, *C. crescentus* lives in dilute aquatic environments where cell dispersal and exploration of new environments for nutrients largely relies on motility. Mathematical models predict that cell shape affects the swimming and environmental sensing prop-

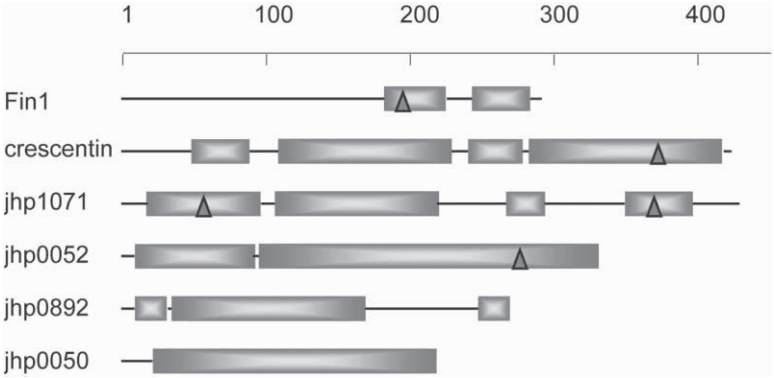

Figure 6. Predicted Coiled-Coil Domain Organization of *Helicobacter pylori* Candidate Proteins for an IF-Like Function

The molecular architecture of yeast IF protein Fin1, crescentin, and 4 uncharacterized coiled-coil proteins from *H. pylori* J99 is depicted. The numbers on the scale represent amino acid residues. Coiled-coil regions and stutters are indicated as gray rectangles and triangles, respectively.

erties of motile bacteria (Dusenbery, 1998). Because *C. crescentus* cells are propelled by a helical flagellum located at one cell pole, it is likely that the curvature of these cells affects the swimming path and the three-dimensional sampling of the environment, which in nature has considerable importance.

How Represented Is the IF-Like Cytoskeletal Function across Kingdoms?

IF proteins have been identified almost exclusively in animals, with a few exceptions. All metazoan IF proteins described to date have the stereotyped segmented coiled-coil domain structure illustrated in Figure 4. The *Saccharomyces cerevisiae* genome has no predicted ORF with a coiled-coiled domain organization comparable to metazoan IF proteins (Mewes et al., 1998). The characterized yeast IF protein Fin1 has a different organization of extended coiled-coil motifs (Figure 6) (Mayordomo and Sanz, 2002; van Hemert et al., 2002, 2003), suggesting that various arrangements of coiled-coil regions may give rise to similar IF-like biochemical properties. With this in mind, we analyzed several genome sequences of curved and helical bacteria using the COILS algorithm to identify coiled-coil proteins that may be candidates for an IF-like cytoskeletal role (see Experimental Procedures). A BLAST search using crescentin as a query also identified coiled-coil proteins but this search was markedly biased toward proteins containing large regions of uninterrupted coiled-coils. From the set of coiled-coil proteins obtained with the COILS program, we eliminated proteins with annotated functions and those with predicted transmembrane domains or signal peptide sequences. Using these criteria, putative candidates for an IF-like role were identified from each bacterial genome analyzed. Figure 6 shows the candidate coiled-coil proteins for *Helicobacter pylori*. In plants, no IF protein has been described thus far. A recent genomic study aimed to investigate coiled-coil proteins from *Arabidopsis* did not find proteins with the same domain organization as animal IF proteins. However, the same study identified a family of uncharacterized proteins with extended coiled-coils (named filament-like plant proteins), some members of which may fulfill an IF-like function (Gindullis et al., 2002). Biochemical and functional studies on coiled-coil proteins from diverse bacte-

Table 1. Strains and Plasmids

Strain	Description	Source
C. crescentus		
CB15N	Wild-type strain, also named NA1000	(Evinger and Agabian, 1977)
CJW578	Used for Tn5 mutagenesis; contains two fluorescently labeled proteins (DivJ-CFP and DivK-YFP)	This study
CJW761	Tn5 insertion mutant of CJW578	This study
CJW762	Tn5 insertion mutant of CJW578	This study
CJW763	CB15N *creS*::Tn5	This study
CJW932	CB15N *creS::creS-flag; creS* is replaced by *creS-flag*	This study
CJW934	CB15N *creS::creS-gfp*; *creS* is replaced by *creS-gfp*	This study
CJW935	CB15N *creS::gfp-creS; creS* is replaced by *gfp-creS*	This study
CJW815	Merodiploid strain containing both *creS* and *creS-gfp* integrated at the *creS* locus	This study
CJW935	Merodiploid strain containing both *creS* and *gfp-creS* integrated at the *creS* locus	This study
E. coli		
DH5α	Cloning strain	Promega
S17-1	RP4-2, Tc::Mu Km::Tn7; for plasmid mobilization	(Simon et al., 1983)
BL21(DE3)	F^- *ompT* $hsdS_B(rB^- mB^-)$ *dcm gal* (DE3); for protein overexpression	Novagen
Plasmids	**Description**	**Source**
pMR20	Broad host range cloning vector	(Roberts et al., 1996)
pMR20CreS	pMR20 carrying full-length wild-type *creS*	This study
pET-28a(+)	Vector for protein overexpression	Novagen
pET28-CreS	pET-28a(+) carrying *creS* for expression of His-CreS	This study

ria, fungi, and plants will be very interesting as they may inform us about the relatedness between these proteins and metazoan IF proteins.

Importantly, IF proteins had been missing from the known assortment of bacterial cytoskeletal proteins, which includes the previously described actin and tubulin-related proteins (Bi and Lutkenhaus, 1991; Jones et al., 2001; Lowe and Amos, 1998; Moller-Jensen et al., 2002; van den Ent et al., 2001, 2002). The discovery of IF-like crescentin filaments in *C. crescentus* shows that all three types of major intracellular filaments found in animals are represented in the prokaryotic kingdom.

Experimental Procedures

Bacterial Strains, Plasmids, and Growth

Strains and plasmids are listed in Table 1. *C. crescentus* strains were grown in peptone-yeast extract complex media (PYE) at 28°C (Ely, 1991). Plasmids were introduced into *C. crescentus* strains by bacterial conjugation using mobilization by *E. coli* strain S17-1 (Ely, 1991). The mode of construction of strains and plasmids, as well as the sequences of all primers, are available upon request.

Tn*5* Mutagenesis

A Tn*5* derivative, mini Tn5 Km2 (de Lorenzo et al., 1990; Herrero et al., 1990), was used to mutagenize strain CJW578. Tn*5* insertion mutants were visually screened for cell morphology defects by DIC microscopy. The original Tn*5* mutation in strain CJW761 was transferred into wild-type CB15N by ϕCR30 phage transduction (Ely, 1991).

Light Microscopy

A Nikon E1000 microscope equipped with a DIC 100× objective and a Hamamatsu Orca-ER LCD camera was used for DIC and fluorescence imaging. Live cells were immobilized on slides covered with 1% agarose in M2G minimal medium (Ely, 1991) and observed at room temperature. Cell membranes were visualized using the lipophilic fluorescent dye FM 4-64 (Molecular Probes, OR) at a final concentration of 4 μg/ml. Immunofluorescence microscopy was performed as described previously (Domian et al., 1997) using an anti-FLAG antibody (Zymed Labs, CA) at a dilution of 1:100. Images were taken with Metamorph software (Universal Imaging, PA).

In Vitro Filament Formation and Electron Microscopy

N terminally polyhistidine-tagged crescentin (His-CreS) expressed from the pET-28a(+) vector in *E. coli* BL21(DE3) was purified using the BD TALON Metal Affinity Resin (BD Biosciences Clontech, CA) under denaturing conditions (6 M guanidinium) as described in the user manual. The protein preparation was dialyzed against 30 mM Tris-HCl, pH 8.4 in 6 M guanidinium. To induce filament formation, protein samples (0.5 mg/ml) were dialyzed against 50 mM Tris-HCl, pH 7.0 for 2 hr at room temperature (with one bath change). The dialyzed samples were then applied on glow discharge carbon-coated grids, negatively stained with 1% uranyl acetate, and viewed on a Zeiss EM 10A electron microscope (80 kV).

Deconvolution and Image Processing

Point-spread functions (PSF) were measured using 175 nm fluorescent beads (Point Source Kit, Molecular Probes, OR) immobilized on slides with a 1% agarose pad and imaged under conditions similar to those for bacteria. Ten beads were measured at each wavelength and averaged to obtain each PSF. Three-dimensional deconvolution was performed with a custom software package (J.R.K.) implementing the expectation maximum iterative deconvolution algorithm (Conchello and McNally, 1996). Stack slices were spaced 100 nm apart and 2000 iterations proved sufficient to remove most out-of-focus information. Batch processing of image stacks, calculation of PSF stacks, and 3D reconstruction of deconvolved stacks were performed with custom plug-ins (J.R.K.) for the public domain image analysis program, ImageJ (U.S. National Institutes of Health). Three-dimensional projections were calculated using a maximum intensity projection and stereo pairs were separated by 9°. Stack acquisition, measurement of the CreS-GFP helix parameters, 2D deconvolution of image stacks, and all other image processing were performed with Metamorph (Universal Imaging, PA). The schematic representation of the helical *C. crescentus* cell containing a left-handed helical crescentin structure running along the shortest helical path was produced in Mathematica (Wolfram Research, Champaign, IL, USA) using the following measured parameters: cell thickness of 1.1 μm, helical path with the pitch of 9.2 μm, and diameter of 3.7 μm.

Database Searches

Using the COILS algorithm (Lupas, 1996), coiled-coil proteins were identified from the genomes of *Rhodospirillum rubrum*, *Geobacter metallireducens*, *Campylobacter jejuni*, *Helicobacter pylori* strain J99, *Helicobacter hepaticus* strain ATCC 51449, *Vibrio cholerae*, *Vibrio parahaemolyticus*, *Pasteurella multocida*, *Borrelia burgdorferi*, and *Treponema pallidum*.

Each protein with over 80 amino acid residues in predicted coiled-coil conformation was further analyzed using the DAS transmembrane prediction (Cserzo et al., 1997) and SignalP (Nielsen et al., 1997) algorithms to discard proteins with a signal peptide sequence or a predicted transmembrane domain. The putative function of the remaining coiled-coil proteins was investigated using BLAST (basic local alignment search tool; Altschul et al., 1997); only proteins with no associated function were kept as candidates for a putative IF-like role.

The predicted locations of stutters (corresponding to the omission of 3 residues from the heptad pattern) were determined using the COILS algorithm with a scanning window of 28 residues (Lupas, 1996).

Acknowledgments

We thank Thomas Pollard, Mark Mooseker, and the members of the Jacobs-Wagner laboratory for critical reading of the manuscript. We are also grateful to Mark Mooseker and Barry Piekos for their advice on electron microscopy. We thank David Kysela for his help with the genome database searches. This work was supported by National Institutes of Health grants GM065835 (C.J.-W.) and GM26338 (T.D. Pollard), the Pew Scholars Program in the Biological Sciences sponsored by the Pew Charitable Trusts (C.J.-W.), a Yale Endowed Postdoctoral Fellowship (N.A.), and a Career Award at the Scientific Interface from the Burroughs Wellcome Fund (J.R.K.).

Received: September 3, 2003
Revised: November 12, 2003
Accepted: November 12, 2003
Published: December 11, 2003

References

Altschul, S.F., Madden, T.L., Schaffer, A.A., Zhang, J., Zhang, Z., Miller, W., and Lipman, D.J. (1997). Gapped BLAST and PSI-BLAST: a new generation of protein database search programs. Nucleic Acids Res. *25*, 3389–3402.

Bi, E.F., and Lutkenhaus, J. (1991). FtsZ ring structure associated with division in *Escherichia coli*. Nature *354*, 161–164.

Bork, P., Sander, C., and Valencia, A. (1992). An ATPase domain common to prokaryotic cell cycle proteins, sugar kinases, actin, and hsp70 heat shock proteins. Proc. Natl. Acad. Sci. USA *89*, 7290–7294.

Brown, J.H., Cohen, C., and Parry, D.A. (1996). Heptad breaks in alpha-helical coiled coils: stutters and stammers. Proteins *26*, 134–145.

Carballido-Lopez, R., and Errington, J. (2003). The bacterial cytoskeleton: in vivo dynamics of the actin-like protein Mbl of *Bacillus subtilis*. Dev. Cell *4*, 19–28.

Conchello, J.-A., and McNally, J.G. (1996). Fast regularization technique for expectation maximization algorithm for optical sectioning microscopy. In Three-Dimensional Microscopy: Image Acquisition

and Processing III, C.J. Cogswell, G.S. Kino, and T. Wilson, eds. (April, 1996: www.spie.org) pp. 199–208.

Cserzo, M., Wallin, E., Simon, I., von Heijne, G., and Elofsson, A. (1997). Prediction of transmembrane alpha-helices in prokaryotic membrane proteins: the dense alignment surface method. Protein Eng. *10*, 673–676.

Daniel, R.A., and Errington, J. (2003). Control of cell morphogenesis in bacteria: two distinct ways to make a rod-shaped cell. Cell *113*, 767–776.

de Lorenzo, V., Herrero, M., Jakubzik, U., and Timmis, K.N. (1990). Mini-Tn5 transposon derivatives for insertion mutagenesis, promoter probing, and chromosomal insertion of cloned DNA in gram-negative eubacteria. J. Bacteriol. *172*, 6568–6572.

Domian, I.J., Quon, K.C., and Shapiro, L. (1997). Cell type-specific phosphorylation and proteolysis of a transcriptional regulator controls the G1-to-S transition in a bacterial cell cycle. Cell *90*, 415–424.

Domingo, A., Sarria, A.J., and Evans, R.M. and Klymkowsky, M.W. (1992). Studying intermediate filaments. In The Cytoskeleton; A Practical Approach, K.L. Carraway, and C.A.C. Carraway, eds. (Oxford, IRL Press), pp. 223–255.

Dusenbery, D.B. (1998). Fitness landscapes for effects of shape on chemotaxis and other behaviors of bacteria. J. Bacteriol. *180*, 5978–5983.

Ely, B. (1991). Genetics of *Caulobacter crescentus*. Methods Enzymol. *204*, 372–384.

Evinger, M., and Agabian, N. (1977). Envelope-associated nucleoid from *Caulobacter crescentus* stalked and swarmer cells. J. Bacteriol. *132*, 294–301.

Gindullis, F., Rose, A., Patel, S., and Meier, I. (2002). Four signature motifs define the first class of structurally related large coiled-coil proteins in plants. BMC Genomics *3*, 1–11.

Henning, U., Rehn, K., Braun, V., and Hohn, B. (1972). Cell envelope and shape of *Escherichia coli* K12. Properties of a temperature-sensitive rod mutant. Eur. J. Biochem. *26*, 570–586.

Henriques, A.O., Glaser, P., Piggot, P.J., and Moran, C.P., Jr. (1998). Control of cell shape and elongation by the *rodA* gene in *Bacillus subtilis*. Mol. Microbiol. *28*, 235–247.

Herrero, M., de Lorenzo, V., and Timmis, K.N. (1990). Transposon vectors containing non-antibiotic resistance selection markers for cloning and stable chromosomal insertion of foreign genes in gram-negative bacteria. J. Bacteriol. *172*, 6557–6567.

Herrmann, H., Haner, M., Brettel, M., Ku, N.O., and Aebi, U. (1999). Characterization of distinct early assembly units of different intermediate filament proteins. J. Mol. Biol. *286*, 1403–1420.

Huiatt, T.W., Robson, R.M., Arakawa, N., and Stromer, M.H. (1980). Desmin from avian smooth muscle. Purification and partial characterization. J. Biol. Chem. *255*, 6981–6989.

Ip, W., Hartzer, M.K., Pang, Y.Y., and Robson, R.M. (1985). Assembly of vimentin in vitro and its implications concerning the structure of intermediate filaments. J. Mol. Biol. *183*, 365–375.

Jones, L.J., Carballido-Lopez, R., and Errington, J. (2001). Control of cell shape in bacteria: helical, actin-like filaments in *Bacillus subtilis*. Cell *104*, 913–922.

Kruse, T., Moller-Jensen, J., Lobner-Olesen, A., and Gerdes, K. (2003). Dysfunctional MreB inhibits chromosome segregation in *Escherichia coli*. EMBO J. *22*, 5283–5292.

Lowe, J., and Amos, L.A. (1998). Crystal structure of the bacterial cell-division protein FtsZ. Nature *391*, 203–206.

Lupas, A. (1996). Prediction and analysis of coiled-coil structures. Methods Enzymol. *266*, 513–525.

Lupas, A., Van Dyke, M., and Stock, J. (1991). Predicting coiled coils from protein sequences. Science *252*, 1162–1164.

Mayordomo, I., and Sanz, P. (2002). The *Saccharomyces cerevisiae* 14–3-3 protein Bmh2 is required for regulation of the phosphorylation status of Fin1, a novel intermediate filament protein. Biochem. J. *365*, 51–56.

Mewes, H.W., Hani, J., Pfeiffer, F., and Frishman, D. (1998). MIPS: a database for protein sequences and complete genomes. Nucleic Acids Res. *26*, 33–37.

Moller-Jensen, J., Jensen, R.B., Lowe, J., and Gerdes, K. (2002). Prokaryotic DNA segregation by an actin-like filament. EMBO J. *21*, 3119–3127.

Nelson, D.E., and Young, K.D. (2000). Penicillin binding protein 5 affects cell diameter, contour, and morphology of *Escherichia coli*. J. Bacteriol. *182*, 1714–1721.

Nielsen, H., Engelbrecht, J., Brunak, S., and von Heijne, G. (1997). Identification of prokaryotic and eukaryotic signal peptides and prediction of their cleavage sites. Protein Eng. *10*, 1–6.

Renner, W., Franke, W.W., Schmid, E., Geisler, N., Weber, K., and Mandelkow, E. (1981). Reconstitution of intermediate-sized filaments from denatured monomeric vimentin. J. Mol. Biol. *149*, 285–306.

Roberts, R.C., Toochinda, C., Avedissian, M., Baldini, R.L., Gomes, S.L., and Shapiro, L. (1996). Identification of a *Caulobacter crescentus* operon encoding *hrcA*, involved in negatively regulating heat-inducible transcription, and the chaperone gene *grpE*. J. Bacteriol. *178*, 1829–1841.

Rost, B., and Sander, C. (1993). Prediction of protein secondary structure at better than 70% accuracy. J. Mol. Biol. *232*, 584–599.

Shih, Y.-L., Le, T., and Rothfield, L. (2003). Division site selection in *Escherichia coli* involves dynamic redistribution of Min proteins within coiled structures that extend between the two cell poles. Proc. Natl. Acad. Sci. USA *100*, 7865–7870.

Shohayeb, M., and Chopra, I. (1987). Mutations affecting penicillin-binding proteins 2a, 2b and 3 in *Bacillus subtilis* alter cell shape and peptidoglycan metabolism. J. Gen. Microbiol. *133*, 1733–1742.

Simon, R., Prieffer, U., and Puhler, A. (1983). A broad host range mobilization system for in vivo genetic engineering: transposon mutagenesis in gram negative bacteria. Biotechnology *1*, 784–790.

Spratt, B.G. (1975). Distinct penicillin binding proteins involved in the division, elongation, and shape of *Escherichia coli* K12. Proc. Natl. Acad. Sci. USA *72*, 2999–3003.

Steinert, P.M., Idler, W.W., and Zimmerman, S.B. (1976). Self-assembly of bovine epidermal keratin filaments in vitro. J. Mol. Biol. *108*, 547–567.

Strelkov, S.V., Herrmann, H., Geisler, N., Wedig, T., Zimbelmann, R., Aebi, U., and Burkhard, P. (2002). Conserved segments 1A and 2B of the intermediate filament dimer: their atomic structures and role in filament assembly. EMBO J. *21*, 1255–1266.

Strelkov, S.V., Herrmann, H., and Aebi, U. (2003). Molecular architecture of intermediate filaments. Bioessays *25*, 243–251.

Tamaki, S., Matsuzawa, H., and Matsuhashi, M. (1980). Cluster of *mrdA* and *mrdB* genes responsible for the rod shape and mecillinam sensitivity of *Escherichia coli*. J. Bacteriol. *141*, 52–57.

Townsend, R., Archer, D.B., and Plaskitt, K.A. (1980). Purification and preliminary characterization of *Spiroplasma fibrils*. J. Bacteriol. *142*, 694–700.

Trachtenberg, S., and Gilad, R. (2001). A bacterial linear motor: cellular and molecular organization of the contractile cytoskeleton of the helical bacterium *Spiroplasma melliferum* BC3. Mol. Microbiol. *41*, 827–848.

Trachtenberg, S., Gilad, R., and Geffen, N. (2003). The bacterial linear motor of *Spiroplasma melliferum* BC3: from single molecules to swimming cells. Mol. Microbiol. *47*, 671–697.

van den Ent, F., Amos, L.A., and Lowe, J. (2001). Prokaryotic origin of the actin cytoskeleton. Nature *413*, 39–44.

van den Ent, F., Moller-Jensen, J., Amos, L.A., Gerdes, K., and Lowe, J. (2002). F-actin-like filaments formed by plasmid segregation protein ParM. EMBO J. *21*, 6935–6943.

van Hemert, M.J., Lamers, G.E., Klein, D.C., Oosterkamp, T.H., Steensma, H.Y., and van Heusden, G.P. (2002). The *Saccharomyces cerevisiae* Fin1 protein forms cell cycle-specific filaments between spindle pole bodies. Proc. Natl. Acad. Sci. USA *99*, 5390–5393.

van Hemert, M.J., Deelder, A.M., Molenaar, C., Steensma, H.Y., and van Heusden, G.P. (2003). Self-association of the spindle pole body-

related intermediate filament protein Fin1p and its phosphorylation-dependent interaction with 14–3-3 proteins in yeast. J. Biol. Chem. *278*, 15049–15055.

Vollmer, W., and Holtje, J.V. (2001). Morphogenesis of *Escherichia coli*. Curr. Opin. Microbiol. *4*, 625–633.

Wachi, M., Doi, M., Tamaki, S., Park, W., Nakajima-Iijima, S., and Matsuhashi, M. (1987). Mutant isolation and molecular cloning of mre genes, which determine cell shape, sensitivity to mecillinam, and amount of penicillin-binding proteins in *Escherichia coli*. J. Bacteriol. *169*, 4935–4940.

Wortinger, M.A., Quardokus, E.M., and Brun, Y.V. (1998). Morphological adaptation and inhibition of cell division during stationary phase in *Caulobacter crescentus*. Mol. Microbiol. *29*, 963–973.